Regulation of Transient Site-specific Copy Gain by MicroRNA

Joshua C. Black[1], Hailei Zhang[2], Jaegil Kim[2], Gad Getz[2,3], Johnathan R. Whetstine[1]*

[1] Massachusetts General Hospital Cancer Center and Department of Medicine, Harvard Medical School, 13th Street, Charlestown, Massachusetts 02129
[2] Broad Institute of MIT and Harvard, Cambridge, Massachusetts 02142
[3] Massachusetts General Hospital Cancer Center and Department of Pathology, Harvard Medical School, 13th Street, Charlestown, Massachusetts 02129

Running Title: *MicroRNA Regulation of TSSG*

To whom correspondence should be addressed: Johnathan R Whetstine, Department of Medicine, Harvard Medical School and Massachusetts General Hospital Cancer Center, Room 7-213 Bldg. 149 13th Street, Charlestown, Massachusetts, 02129, Telephone: (617) 643-4347; FAX: (617) 724-9648; E-mail: jwhetstine@hms.harvard.edu

Abstract

Intra-tumor copy number heterogeneity is commonly observed in cancer, however the molecular mechanisms that contribute to heterogeneity remain poorly understood. Upregulation of the histone demethylase KDM4A promotes transient site-specific copy gain (TSSG) in cells; therefore, uncovering how KDM4A levels are controlled is important to understanding the regulation of copy number heterogeneity. Here, we demonstrate that KDM4A is regulated by hsa-mir-23a-3p, hsa-mir-23b-3p and hsa-mir-137. Altering expression of these miRNAs regulates KDM4A-dependent TSSG. miRNA inhibition promoted copy gains and increased expression of the drug resistant oncogene *CKS1B*, which was further substantiated in primary breast tumors. Consistent with increased *CKS1B* expression, miRNA inhibition reduced breast cancer cell sensitivity to cisplatin. Our data identify these miRNAs as regulators of TSSG and copy gains of a drug resistance gene.

Introduction

Genomic instability is a hallmark of cancer and contributes to drug resistance (1). Both adult and pediatric cancers have recurrent gains and losses of chromosomal regions, but little is known regarding the molecular mechanisms causing either transient or permanent copy number changes at specific sites within the genome. Such copy number gains, when contributing to increased expression of oncogenes, have been shown to impact cellular behavior and/or correlate with poor outcome and reduced chemotherapeutic response (2-5). For instance, tumors with worse outcome and reduced response to therapeutics often harbor chromosome 1q12-25 cytogenetic gains; however, the genes that contribute to this phenotype may vary depending on tumor type even though the same cytogenetic region is gained (2-10).

We previously discovered that overexpression of the lysine demethylase KDM4A/JMJD2A and the modulation of epigenetic states (i.e., histone 3 lysine 9 and 36 methylation) results in transient site-specific copy gains (TSSGs) through rereplication in the human genome (11-13).

TSSGs are copy gain/amplification events that are reversible, occur during cell cycle, but are not permanently integrated into the genome (11-13). Overexpression of histone lysine demethylase KDM4A was sufficient to promote rereplication and copy gain of specific chromosomal regions that are implicated in drug resistance and worse clinical outcome (*e.g.*, 1q12h and 1q21) (2-5,11-13). The *KDM4A* locus (1p34.1) is amplified in human tumors (~20%) and significantly correlates with copy gains that were recapitulated as TSSGs in transgenic cell lines (12). Moreover, TSSG is not just a cancer specific event, but can be regulated by physiologic stimuli. For example, hypoxia also promotes TSSGs through stabilization of KDM4A protein levels (11,13). Thus, understanding how KDM4A is regulated will help understand TSSGs, intra-tumor copy number heterogeneity and provide insights into the amplification of potential drug resistance genes, especially in the 1q12-21 locus.

KDM4A protein levels are regulated, during cell cycle and in hypoxic exposure, by the SKP1-Cul1-F-box ubiquitin ligase complex and at least three F-box proteins (11,14-17). However, it is likely that other mechanisms exist to modulate KDM4A protein levels, which will play an important role in regulating TSSG in 1q12-21. Possible candidates for regulating KDM4A are microRNAs (miRNAs). MicroRNAs are short (19-22 nucleotides) non-coding RNAs, which in complex with the RNA-induced silencing complex (RISC) target the 3'-untranslated region (3'-UTR) through binding to specific complementary seed sequences (18). Transcripts targeted by RISC/miRNA are then translationally repressed or degraded (18).

Here, we demonstrate that KDM4A is regulated by hsa-mir-23a/b-3p (hereafter hsa-mir-23a/b) and hsa-mir-137. Addition of miRNA mimics to cells resulted in decreased KDM4A protein expression, while inhibition of the endogenous miRNA resulted in increased KDM4A protein levels. Addition of

the KDM4A 3'-UTR to luciferase rendered it responsive to these miRNA, which was blocked by mutation of the hsa-mir-23a/b and hsa-mir-137 seed sequences. Interestingly, upregulation of KDM4A through depletion of these miRNA promotes TSSG of 1q12-21. Reciprocally, treatment with hsa-mir-23a/b or hsa-mir-137 mimics was sufficient to abrogate KDM4A-dependent TSSGs in response to hypoxia. Consistent with these observations, we used miRNA inhibitors in MDA-MB-231 breast cancer cells to promote gain of 1q12-21 as well as the amplification and increased expression of *CKS1B*, which is a drug resistant oncogene *(4,19-22)*. Furthermore, analysis of primary breast tumors (BRCA) in The Cancer Genome Atlas (TCGA) revealed that deletion of hsa-mir-23a correlates with increased copy number of 1q12-21 in primary tumors and associates with copy gain and increased expression of the drug resistant oncogene *CKS1B*. Consistent with these observations, miRNA inhibitors reduced breast cancer cell response to cisplatin. Our results implicate miRNA regulation as a modulator of TSSGs and suggest that miRNA therapy could be used to reduce KDM4A-driven copy number heterogeneity and potentially affect drug resistance.

Experimental Procedures

Cell Culture and Transfections— hTERT-RPE-1 (called RPE throughout manuscript) and MDA-MB-231, cells were maintained in DMEM with 10% fetal bovine serum, 1% penicillin/streptomycin, and L-glutamine. SK-N-AS cells were maintained in DMEM/F12 (Gibco) with 10% fetal bovine serum, 1% penicillin/streptomycin, and L-glutamine. H2591 cells were maintained in RPMI (Gibco) with 10% fetal bovine serum, 1% penicillin/streptomycin, and L-glutamine. Transient transfection experiments with miRNA mimics or inhibitors were performed using Roche X-tremeGENE siRNA reagent in OPTI-MEM I media overnight (approximately 12 hours). Media was changed to DMEM (or DMEM/F12 or RPMI as appropriate) following the overnight

incubation and cells were collected at 72 hours following transfection. Each miRNA experiment represents the average of at least two different transfections for each miRNA mimic or inhibitor. Transient transfection experiments with KDM4A siRNA were co-transfected with the miRNA using Roche X-tremeGENE siRNA reagent in OPTI-MEM I media overnight. Silencer Select siRNA for KDM4A was purchased from Life Technologies (s18636).

Hypoxic Conditions—Cells were plated onto culture dishes and allowed to adhere for 20-24 hours in normoxia (5% CO_2, 21% O_2, and 74% N_2). For hypoxic treatment, cells were maintained in a HERA Cell 150 incubator (Thermo Scientific) flushed with 5% CO_2, 1% O_2, and balanced with N_2 for the duration of the experiment. Incubator calibrations and verifications were carried out by Bianchi Associates Calibrations/Verifications.

Fluorescent In Situ Hybridization (FISH)—FISH was performed as described in (12). Probes for 1q12h, chromosome 8 centromere (alpha satellite) and *CKS1B* were purchased from Rainbow Scientific through Oxford Gene Technologies. Probes for 1q21.2 (*BCL9*) and 1q23.3 were purchased from Agilent (SureFISH). Images of multiple planes of fields of nuclei were acquired on an Olympus IX81 Spinning Disk Microscope using a 40X objective and analyzed using Slidebook 5.0 software. We used a conservative scoring metric for copy gain. Any foci that were touching were scored as a single copy to prevent increased numbers due to normally replicated foci. For RPE cells, copy gain was scored as any cell with 3 or more distinct foci. For MDA-MB-231 cells, copy gain was scored for any cell with 7 or more foci for 1q12h and *CKS1B* and 5 or more for 8c or *CDKN2C*. For SK-N-AS cells copy gain was scored for any cell with 4 or more foci for 1q12h 3 or more for 8c. . For H2591 cells copy gain was scored for any cell with 5 or more foci for 1q12h 4 or more for 8c. Approximately 100 cells for each replicate were scored for all experiments. All

FISH experiments include at least 2 biological replicates.

Antibodies—Antibodies used were: KDM4A (Neuro mAB, 75-189), β-actin (Millipore), Actinin (Santa Cruz, sc-17829), CAIX (Abcam, ab108351).

Western Blots—Western blots were performed as in (14). Samples for western analysis were from the same collections used for FISH, FACS and RNA analyses. Quantitation was performed using ImageJ gel analysis with area under the curve. KDM4A levels were normalized to Actin or Actinin levels (as indicated in each figure) and then a ratio to the appropriate control sample was calculated. Data are thus presented as a fold change relative to the control.

Expression plasmids and luciferase assays—The WT and MT KDM4A 3'-UTR were cloned into pMIR as the 3'-UTR to luciferase. The pMIR-3'-UTR constructs and a β-galactosidase construct for normalization were co-transfected with the indicated miRNA mimics for 48 hours using Roche xTremeGene siRNA transfection reagent (Roche) in OPTI-mem I media (Life Technologies). Cells were collected by scraping and lysates were prepared following the Dual-Light system instructions (Life Technologies). The dual luciferase and Beta-galactosidase assays were performed using the Dual-Light system following the manufacturer's instructions (Life Technologies). Measurements for two biological replicates were taken in triplicate and averaged.

miRNA mimics and inhibitors—The miRNA mimics and inhibitors were purchased from Life Technologies. The mimics used were MirVana pre-miRNA23a (MC10644), MirVana pre-miRNA23b (MC10711), MirVana pre-miRNA137 (MC10513), MirVana pre-miRNA200b (MC10492), and MirVana pre-miRNA200c (MC11714) and MirVana Control (4464058). The inhibitors used were MiRVana anti-

miRNA23a (MH10644), MiRVana anti-miRNA23b (MH10711), MiRVana anti-miRNA137 (MH10513), MiRVana anti-miRNA200b (MH10492), MiRVana anti-miRNA200c (MH11714), and MirVana Control (4464076).

Cisplatin sensitivity by MTT assay—5000 MDA-MB-231 cells were plated overnight in each well of a 96 well plate. Cells were transfected with miRNA inhibitors using Roche X-tremeGENE siRNA reagent in OPTI-MEM I media overnight (approximately 12 hours). Media was changed to DMEM following the overnight incubation and cells were allowed to recover for eight hours. Cisplatin (abcam ab 141398) was resuspended in 0.9% NaCl right before use. Cisplatin was added following the eight hour recovery to a final concentration of 300 μM. Cells were processed using Cell Proliferation Kit I MTT (Roche) 48 hours after addition of cisplatin following the manufacturer's instructions. Each experiment consisted of four technical replicate wells that were averaged together and then taken as a ratio to the no cisplatin sample. The data presented are the average of eight biological replicates.

RNA Extraction and Quantitative PCR—RNA extraction, cDNA synthesis and quantitative PCR were conducted as in (11). Expression levels were analyzed by quantitative real time PCR in a Lightcycler 480 with FastStart Universal SYBR Green Master (Roche) following the manufacturer's protocols. All samples were normalized by comparison to β-actin transcript levels. Primers available upon request.

TCGA Data Set and Copy Number Determination—The copy number and mRNA expression for TCGA Breast Cancer (BRCA) were download from Broad GDAC (Genome Data Analysis Center) Firehose analysis run of 2014_07_15 (doi:10.7908/C1TQ60P0). 1,030 common samples from two data platforms were used in this analysis. The somatic copy number alterations (SCNAs) for 23,246 genes and

928 microRNAs were annotated by GISTIC2.0 (23-25). The copy number change in each gene/miRNA is defined as possessing deep deletion (-2), shallow deletions (-1), neutral copy number (0), low gain (+1), and high gain (+2) in each sample using sample-specific thresholds. High gains are segments with copy number that exceed the maximum median chromosomal arm copy number for that sample by at least 0.1; low gains are segments with copy numbers from 2.1 to the high gain threshold; neutral segments have copy numbers between 1.9 and 2.1; shallow losses have copy numbers between 1.9 and the deep deletion threshold; and deep deletion have copy numbers that are below the minimum median chromosomal arm copy number for that sample by at least 0.1.

Determination of Cytoband Copy Number and Correlation with microRNA loss—In addition to the copy number annotation for each gene, the mean focal copy number for 807 cytobands including the X chromosome were annotated in each sample by taking an average of focal copy numbers of every genes within the same cytoband. Arm-level SCNA contributions to the mean focal copy number in each cytoband were removed by only considering GISTIC annotated focal copy numbers that are smaller than a chromosome arm or entire chromosome. Detecting chromosomal regions significantly co-amplified with microRNA copy loss or deletion was performed by approximating a null distribution of mean cytoband copy differences by a normal function $N(\mu_{12} - \mu_0, \frac{\sigma_0^2}{n_0} + \frac{\sigma_{12}^2}{n_{12}})$ where μ_0 and μ_{12} are samples means across all cytobands, σ_0^2 and σ_{12}^2 are mean sample-specific variances with each group, and n_0 and n_{12} are the number of samples in microRNA copy-neutral (GISTIC annotation = 0) and microRNA copy-loss (GISTIC annotation = -1 or -2) groups, respectively. This test is based on comparing the means of the two sets while permuting values within each of the samples (and

using a Gaussian approximation). The p-values across 807 cytobands were annotated by computing the probability of more extreme differences than the corresponding cytoband copy difference in the null distribution. The QQ plot of those p-values is used to show that many genes follow the null hypothesis and their associated p-values behave appropriately.

Results

KDM4A is regulated by miRNAs— KDM4A is an important regulator of TSSGs (11-13). Uncovering how KDM4A protein levels are regulated is crucial to understanding how TSSGs can be regulated. KDM4A levels are largely regulated post-transcriptionally (11,12,14-17), suggesting that miRNAs may be ideal candidates to contribute to this regulation. To address this hypothesis, we analyzed the TARGETSCAN database for miRNAs that could target KDM4A. TARGETSCAN6.2 identified three conserved miRNA seed sequences in the *KDM4A* 3'-UTR (Fig. 1A) for hsa-mir-23a/b-3p (hereafter hsa-mir-23a/b), hsa-mir-137, and hsa-mir200b/c (26,27). To determine whether these miRNA could indeed regulate KDM4A, we treated the immortalized but non-transformed human retinal pigment epithelial cell line (RPE cells) with miRNA mimics (Fig. 1B). KDM4A protein levels were downregulated when cells were exposed to hsa-mir-23a/b and hsa-mir-137, but had minimal change when exposed to increased hsa-mir200b/c. Moreover, KDM4A protein levels increased when cells were treated with inhibitors of hsa-mir-23a/b and hsa-mir-137, but not with hsa-mir200b/c (Fig. 1C). These results are consistent with hsa-mir-23a/b and hsa-mir-137 regulating KDM4A in human cells.

In order to determine if the *KDM4A* 3'-UTR was the direct target of hsa-mir-23a/b and hsa-mir-137, we cloned the *KDM4A* 3'-UTR downstream of the luciferase cDNA. The miRNA seed sequences were left intact (WT UTR), or carried a series of point mutations removing the seed sequences for

hsa-mir-23a/b, hsa-mir-137 and hsa-mir 200b/c (MT UTR; Fig. 1A). These constructs were then introduced into RPE cells in conjunction with mimics to hsa-mir-23a/b, hsa-mir-137, hsa-mir200b/c or a control miRNA mimic. Cells treated with hsa-mir-23a/b or hsa-mir-137 miRNA reduced luciferase expressions when luciferase was fused with the WT 3'-UTR, but not when attached to the mutated 3'-UTR (MT; Fig. 1D). Overexpression of hsa-mir200b/c did not induce significant change in luciferase expression. Taken together, our data demonstrate that KDM4A is a direct target for regulation by hsa-mir-23a/b and hsa-mir-137 in RPE cells.

Regulation of TSSGs by miRNA— We previously demonstrated that increased expression of KDM4A was sufficient to promote TSSGs (11,12). TSSGs are characterized by cells with at least one additional copy of specific genomic loci that occur during S phase (11-13). The ability of miRNAs to regulate KDM4A protein levels suggested that decreasing hsa-mir-23a/b or hsa-mir-137 expression would be sufficient to increase KDM4A levels and thus promote TSSGs. Therefore, we introduced hsa-mir-23a/b or hsa-mir-137 inhibitors (anti-miRs) into RPE cells for 72 hours and assessed copy number by fluorescent in situ hybridization (DNA-FISH). The anti-miRs were sufficient to induce increased expression of KDM4A (Fig. 2A) without altering cell cycle distribution (Fig. 2B). We then determined the percentage of cells in the population that had at least one additional copy of the regions known to undergo TSSGs (*i.e.* 1q12h and 1q21.2) as well as control regions (*i.e.* 1q23.3 and chromosome 8 centromere) by DNA-FISH. Inhibition of hsa-mir-23a/b or hsa-mir-137 was sufficient to promote copy gain of 1q12h and 1q21.2, but did not alter the copy number of 1q23.3 or chromosome 8 centromere (Fig. 2C-D). We confirmed these findings in MDA-MB-231 breast cancer cells. As in RPE cells, introduction of the anti-miRs resulted in increased KDM4A protein levels (Fig. 2E) without altering steady-state *KDM4A*

transcript levels or cell cycle (Fig. 2F-G). MicroRNA inhibition increased copy number of 1q12h (Fig. 2H), but not the chromosome 8 centromere. Treatment with microRNA inhibitors in neruoblastoma (SK-N-AS cells; Fig 2I-J) and lung cancer cells (H2591; Fig. 2K-L) also increased KDM4A protein levels and promoted copy gain of 1q12h but not chromosome 8 centromere.

TSSGs are characterized by their transient appearance during S phase (11,12). Therefore, we tested whether the observed copy gains were S phase-dependent and by definition TSSGs. RPE cells were transfected with hsa-mir-23a/b or hsa-mir-137 anti-miRs prior to arrest with hydroxyurea (HU) for 20 hrs or arrested and released from HU for four hours. TSSG at 1q12h was assessed by DNA FISH (Fig. 3A-E). Early S arrest with HU blocked the ability of the miRNA inhibitors to induce copy gain (Fig. 3B). However, once cells were released into S phase, hsa-mir-23a/b or hsa-mir-137 anti-miRs promoted copy gain (Fig. 3B). These results demonstrate that inhibition of miRNAs promotes TSSG.

To determine whether the hsa-mir-23a/b or hsa-mir-137 anti-miRs caused TSSG through KDM4A, we co-depleted KDM4A using siRNAs with the KDM4A-targeting anti-miRs. Depletion of KDM4A by siRNA reduced KDM4A levels in the miRNA inhibitor treated cells (Fig. 4A). Cell cycle distribution was unaffected (Fig. 4B), while the reduction in KDM4A levels prevented induction of TSSG by the miRNA inhibitors (Fig. 4C). These results demonstrate that inhibition of hsa-mir-23a/b or hsa-mir-137 promotes TSSG in a KDM4A-dependent manner.

We previously demonstrated that hypoxia could induce TSSGs by stabilizing KDM4A protein levels (11). Since KDM4A protein levels respond to miRNAs, we reasoned that miRNA mimics would deplete KDM4A during hypoxia and prevent hypoxia-induced TSSGs. To test this hypothesis, we transfected RPE cells with miRNA mimics to hsa-mir-23a/b or hsa-mir-137 for 48 hours prior to moving the cells to hypoxia for 24 hours. Introduction of the miRNA mimics was sufficient to blunt the increased expression of KDM4A in hypoxia (Fig. 5A), but did not alter the cell cycle distribution of the treated cells (Fig. 5B). Consistent with the reduction in KDM4A levels, miRNA mimics were sufficient to abrogate hypoxia-dependent TSSG in RPE cells (Fig. 5C). Our results suggest that increasing hsa-mir-23a/b or hsa-mir-137 levels could be effective in reducing hypoxia-induced or KDM4A-dependent TSSG.

Loss of hsa-mir-23a associates with increased CKS1B expression in primary breast tumors—We further substantiated our in vitro findings by analyzing primary breast tumors (BRCA) in The Cancer Genome Atlas (TCGA). Specifically, we evaluated tumors that presented a loss of each miRNA alone and did not present another miRNA loss or *KDM4A* amplification or *KDM4A* loss. Using these criteria, we observed a significant gain for the 1p11.2-1q22 region in tumors presenting a loss for hsa-mir-23a (Fig. 6A). Tumors with loss of the other miRNAs showed a modest significance for this region (hsa-mir-137; Fig. 6B) or no significance (hsa-mir-23b; data not shown). Previously, we demonstrated that breast tumors and breast cancer cells were able to generate copy gain and increased expression of the drug resistant oncogene *CKS1B* (located at 1q21.3 inside the amplified region of tumors with has-mir-23a loss) upon hypoxic exposure (11). We asked if BRCA tumors with hsa-mir-23a loss had increased *CKS1B* expression. We observed that loss of hsa-mir-23a had increased *CKS1B* that was comparable to the increase in expression observed for samples with *KDM4A* amplification (Fig. 6C-D). Loss of hsa-mir-23b or hsa-mir-137 resulted in a comparable trend for increased *CKS1B* expression, but was not significant (data not shown).

6

MicroRNAs regulate copy number and expression of the drug resistant oncogene CKS1B—Copy gain and increased expression of *CKS1B* is associated with poor patient outcome and drug resistant cancer (4,19-22). Understanding mechanisms that can increase *CKS1B* levels has important clinical implications. Since *CKS1B* copy gain and increased expression in hypoxia were KDM4A-dependent, we hypothesized that hsa-mir-23a/b and hsa-mir-137 would promote gain and increased expression for *CKS1B*. In order to directly test this hypothesis, we transfected breast cancer cells (MDA-MB-231) with miRNA inhibitors for hsa-mir-23a, hsa-mir-23b or hsa-mir-137 and assessed copy gain and gene expression. All miRNA inhibitors resulted in increased KDM4A protein levels (Fig 2D), while not altering the cell cycle profile (Fig. 2F). *CKS1B* was gained when cells were treated with hsa-mir-23a/b or hsa-mir-137 anti-miRs and had increased mRNA levels (Fig. 7A-B), which was consistent with our recent findings in hypoxia (11). Since increased copy number and expression of *CKS1B* has been linked to cisplatin resistance (19,22,28,29), we hypothesized that the anti-miR induction would promote resistance to cisplatin in breast cancer cells. Indeed, prior treatment with inhibitors to hsa-mir-23a/b or hsa-mir-137 resulted in decreased sensitivity to cisplatin (Fig. 7C). Taken together, our data demonstrate that miRNAs modulate *CKS1B* gains and expression in vitro and show an association in vivo, which provides another mechanism for increased levels of this oncogene that may contribute to resistance to cisplatin and other drugs in cancer.

Discussion

Our results demonstrate that miRNAs can impact copy number heterogeneity through the regulation of TSSGs by directly regulating a chromatin modifying enzyme. Our data also suggests that other enzymes, transcription factors and environmental conditions cells experience could impact how miRNAs influence copy number gains and expression. Taken together, these findings illustrate the impact that miRNAs could have on transient genome stability through chromatin modulation, which opens a new perspective on how non-coding RNAs could be involved in modulating tumor heterogeneity and potentially promoting phenotypes such as drug resistance. These data also emphasize the need to map the chromatin factors and the miRNAs that regulate them and are involved in TSSGs.

Our data raises the possibility that extrinsic and intrinsic factors could modulate the composition of miRNAs within single cells or a population of cells to control the frequency of TSSGs. Alternatively, cells could alter the 3'-UTR length of key TSSG modulators, and in turn, increase heterogeneity that may impact phenotypes such as drug resistance. It remains possible that altered 3'-UTR length could be important in regulating KDM4A protein levels within tumors since amplification, altered stability and miRNAs are instrumental in regulating KDM4A levels (12,14,16,17). Consistent with this idea, TARGETSCAN7.0 indicates that the *KDM4A* 3'-UTR can use an alternative polyadenylation site that would eliminate the hsa-mir-137 site from the 3'-UTR (Fig. 7D) (30). Loss of the miRNA site from the 3'-UTR could result in increased KDM4A, and in turn, promote TSSGs. Alternatively, cells could select for differential 3'-UTR usage, which is frequently observed in cancer cells (31,32). Differential use of 3'-UTRs without miRNA binding sites could also increase KDM4A levels and promote TSSG and copy number heterogeneity. Future studies need to establish whether *KDM4A* transcripts have altered 3'-UTR lengths that are associated with TSSG-associated copy number heterogeneity.

MicroRNAs are often misregulated in cancer and hsa-mir-23a/b and hsa-mir-137 are no exception (33-40). For example, reduced expression of hsa-mir-137 and hsa-mir-23b has been implicated in cisplatin resistance in solid malignancies (33,36). Consistent with these previous observations,

we observed copy gain and upregulation *of CKS1B*, which is a cell cycle regulator that has been linked to and promotes cisplatin and other drug resistance in myeloma, breast cancer and non-small-cell lung cancer (19,22,28,29). Therefore, tumors carrying the loss of hsa-mir-23a/b and hsa-mir-137 or the mis-regulation of miRNAs could mediate changes in cisplatin response by regulating KDM4A protein levels, promoting transient site-specific copy gains and heterogeneous overexpression of *CKS1B*. For these reasons, it may be beneficial to consider using hsa-mir-23a/b and hsa-mir-137 mimics or *KDM4A* anti-sense RNA strategies to reduce KDM4A protein levels in tumors that have lost these miRNAs or gained *KDM4A*. In fact, miRNA mimics and inhibitors are gaining traction in their use as therapies for metabolic disease and cancer (41,42). As new regulators of TSSGs are identified, it will be important to evaluate how they are regulated and consider miRNAs as a potential way to modulate their activity.

Our work underscores how changes in miRNA abundance could influence how tumors acquire intra-tumoral copy-number heterogeneity. The copy number changes we describe in cell culture models are transient. We observed correlations for these gains in primary tumors; however, future studies need to establish whether the copy number variations associated with miRNA loss in tumors are present in all cancer cells and whether they are transient (*i.e.*, in S-phase only). Most of the miRNA loss events we observed were in the GISTIC (-1) category reflecting low level loss (as opposed, for example, to homozygous deletions) often caused by whole-chromosome or chromosome arm loss. This suggests miRNA loss events are not providing strong fitness advantage to the

cells, but perhaps promote heterogeneity and plasticity that may serve as the basis of future selection. The observed intra-tumoral heterogeneity is likely the result of both permanent and transient heterogeneity. Uncovering how inappropriately amplified regions are lost will help identify pathways that may be mis-regulated in cancer leading to the accumulation and perhaps also inheritance of specific genomic regions. We hypothesize that other defects in cancer cells could then promote incorporation of the TSSGs, and in turn, potentially have a permanent contribution to drug resistance. It still remains to be determined whether TSSGs could, or need to, become permanent and spread across the entire cancer cell population to promote cellular phenotypes such as drug resistance. Therefore, future studies should directly address whether amplified regions in tumors are stable or transient in nature.

In conclusion, this study highlights the important link between chromatin modulation, miRNA levels, heterogeneous and transient site-specific copy-number gains and potential phenotypes such as drug resistance. These findings also reiterate the importance in mapping the pathways and enzymes that are contributing to TSSGs and how the transient overexpression of genes may have a lasting effect on the cancer, even if present only transiently in a subset of the cells (such as potentiating drug resistance). Uncovering these associations will have a profound impact on our understanding of transient copy number heterogeneity and its potential effect on cancer. Ultimately, these networks may identify novel biomarkers and drug targets for cancer genome heterogeneity.

Acknowledgements

Competing Financial Interests

The authors declare competing financial interests: JRW is a consultant for QSonica.

Author Contributions

J.C.B. and J.W. designed the experiments, analyzed data and prepared the manuscript. J.C.B. conducted the experiments in Figures 1- 5 and Figure 7. H.Z., J.K. and G.G. analyzed and prepared figures related to the TCGA analysis in Fig. 6. All authors reviewed the manuscript.

References

1. Hanahan, D., and Weinberg, R. A. (2011) Hallmarks of cancer: the next generation. *Cell* 144, 646-674

2. Dimova, I., Orsetti, B., Theillet, C., Dimitrov, R., and Toncheva, D. (2009) Copy Number Changes in 1q21.3 and 1q23.3 have Different Clinical Relevance in Ovarian Tumors. *Balkan Journal of Medical Genetics* 12, 29-37

3. Diskin, S. J., Hou, C., Glessner, J. T., Attiyeh, E. F., Laudenslager, M., Bosse, K., Cole, K., Mosse, Y. P., Wood, A., Lynch, J. E., Pecor, K., Diamond, M., Winter, C., Wang, K., Kim, C., Geiger, E. A., McGrady, P. W., Blakemore, A. I., London, W. B., Shaikh, T. H., Bradfield, J., Grant, S. F., Li, H., Devoto, M., Rappaport, E. R., Hakonarson, H., and Maris, J. M. (2009) Copy number variation at 1q21.1 associated with neuroblastoma. *Nature* 459, 987-991

4. Fonseca, R., Van Wier, S. A., Chng, W. J., Ketterling, R., Lacy, M. Q., Dispenzieri, A., Bergsagel, P. L., Rajkumar, S. V., Greipp, P. R., Litzow, M. R., Price-Troska, T., Henderson, K. J., Ahmann, G. J., and Gertz, M. A. (2006) Prognostic value of chromosome 1q21 gain by fluorescent in situ hybridization and increase CKS1B expression in myeloma. *Leukemia* 20, 2034-2040

5. Inoue, J., Otsuki, T., Hirasawa, A., Imoto, I., Matsuo, Y., Shimizu, S., Taniwaki, M., and Inazawa, J. (2004) Overexpression of PDZK1 within the 1q12-q22 amplicon is likely to be associated with drug-resistance phenotype in multiple myeloma. *Am J Pathol* 165, 71-81

6. Giulino-Roth, L., Wang, K., MacDonald, T. Y., Mathew, S., Tam, Y., Cronin, M. T., Palmer, G., Lucena-Silva, N., Pedrosa, F., Pedrosa, M., Teruya-Feldstein, J., Bhagat, G., Alobeid, B., Leoncini, L., Bellan, C., Rogena, E., Pinkney, K. A., Rubin, M. A., Ribeiro, R. C., Yelensky, R., Tam, W., Stephens, P. J., and Cesarman, E. (2012) Targeted genomic sequencing of pediatric Burkitt lymphoma identifies recurrent alterations in antiapoptotic and chromatin-remodeling genes. *Blood* 120, 5181-5184

7. Goeze, A., Schluns, K., Wolf, G., Thasler, Z., Petersen, S., and Petersen, I. (2002) Chromosomal imbalances of primary and metastatic lung adenocarcinomas. *J Pathol* 196, 8-16

8. Lestini, B. J., Goldsmith, K. C., Fluchel, M. N., Liu, X., Chen, N. L., Goyal, B., Pawel, B. R., and Hogarty, M. D. (2009) Mcl1 downregulation sensitizes neuroblastoma to cytotoxic chemotherapy and small molecule Bcl2-family antagonists. *Cancer Biol Ther* 8, 1587-1595

9. Vrana, J. A., Bieszczad, C. K., Cleaveland, E. S., Ma, Y., Park, J. P., Mohandas, T. K., and Craig, R. W. (2002) An MCL1-overexpressing Burkitt lymphoma subline exhibits enhanced survival on exposure to serum deprivation, topoisomerase inhibitors, or staurosporine but remains sensitive to 1-beta-D-arabinofuranosylcytosine. *Cancer Res* 62, 892-900

10. Weir, B. A., Woo, M. S., Getz, G., Perner, S., Ding, L., Beroukhim, R., Lin, W. M., Province, M. A., Kraja, A., Johnson, L. A., Shah, K., Sato, M., Thomas, R. K., Barletta, J. A., Borecki, I. B., Broderick, S., Chang, A. C., Chiang, D. Y., Chirieac, L. R., Cho, J., Fujii, Y., Gazdar, A. F., Giordano, T., Greulich, H., Hanna, M., Johnson, B. E., Kris, M. G., Lash, A., Lin, L., Lindeman, N., Mardis, E. R., McPherson, J. D., Minna, J. D., Morgan, M. B., Nadel, M., Orringer, M. B., Osborne, J. R., Ozenberger, B., Ramos, A. H., Robinson, J., Roth, J. A., Rusch, V., Sasaki, H., Shepherd, F., Sougnez, C., Spitz, M. R., Tsao, M. S., Twomey, D., Verhaak, R. G., Weinstock, G. M., Wheeler, D. A., Winckler, W., Yoshizawa, A., Yu, S., Zakowski, M. F., Zhang, Q., Beer, D. G., Wistuba, II, Watson, M. A., Garraway, L. A., Ladanyi, M., Travis, W. D., Pao, W., Rubin, M. A., Gabriel, S. B., Gibbs, R. A., Varmus, H. E., Wilson, R. K., Lander, E. S., and Meyerson,

M. (2007) Characterizing the cancer genome in lung adenocarcinoma. *Nature* 450, 893-898

11. Black, J. C., Atabakhsh, E., Kim, J., Biette, K. M., Van Rechem, C., Ladd, B., Burrowes, P. D., Donado, C., Mattoo, H., Kleinstiver, B. P., Song, B., Andriani, G., Joung, J. K., Iliopoulos, O., Montagna, C., Pillai, S., Getz, G., and Whetstine, J. R. (2015) Hypoxia drives transient site-specific copy gain and drug-resistant gene expression. *Genes Dev* 29, 1018-1031

12. Black, J. C., Manning, A. L., Van Rechem, C., Kim, J., Ladd, B., Cho, J., Pineda, C. M., Murphy, N., Daniels, D. L., Montagna, C., Lewis, P. W., Glass, K., Allis, C. D., Dyson, N. J., Getz, G., and Whetstine, J. R. (2013) KDM4A lysine demethylase induces site-specific copy gain and rereplication of regions amplified in tumors. *Cell* 154, 541-555

13. Black, J. C., and Whetstine, J. R. (2015) Too little O2 Too much gain. *Cell Cycle* 14, 2869-2870

14. Black, J. C., Allen, A., Van Rechem, C., Forbes, E., Longworth, M., Tschop, K., Rinehart, C., Quiton, J., Walsh, R., Smallwood, A., Dyson, N. J., and Whetstine, J. R. (2010) Conserved antagonism between JMJD2A/KDM4A and HP1gamma during cell cycle progression. *Mol Cell* 40, 736-748

15. Tan, M. K., Lim, H. J., and Harper, J. W. (2011) SCF(FBXO22) regulates histone H3 lysine 9 and 36 methylation levels by targeting histone demethylase KDM4A for ubiquitin-mediated proteasomal degradation. *Mol Cell Biol* 31, 3687-3699

16. Van Rechem, C., Black, J. C., Abbas, T., Allen, A., Rinehart, C. A., Yuan, G. C., Dutta, A., and Whetstine, J. R. (2011) The SKP1-Cul1-F-box and leucine-rich repeat protein 4 (SCF-FbxL4) ubiquitin ligase regulates lysine demethylase 4A (KDM4A)/Jumonji domain-containing 2A (JMJD2A) protein. *J Biol Chem* 286, 30462-30470

17. Van Rechem, C., Black, J. C., Greninger, P., Zhao, Y., Donado, C., Burrowes, P. D., Ladd, B., Christiani, D. C., Benes, C. H., and Whetstine, J. R. (2015) A Coding Single Nucleotide Polymorphism in Lysine Demethylase KDM4A Associates with Increased Sensitivity to mTOR Inhibitors. *Cancer Discov*

18. Ha, M., and Kim, V. N. (2014) Regulation of microRNA biogenesis. *Nat Rev Mol Cell Biol* 15, 509-524

19. Khattar, V., and Thottassery, J. V. (2013) Cks1: Structure, Emerging Roles and Implications in Multiple Cancers. *J Cancer Ther* 4, 1341-1354

20. Martin-Ezquerra, G., Salgado, R., Toll, A., Baro, T., Mojal, S., Yebenes, M., Garcia-Muret, M. P., Sole, F., Quitllet, F. A., Espinet, B., and Pujol, R. M. (2011) CDC28 protein kinase regulatory subunit 1B (CKS1B) expression and genetic status analysis in oral squamous cell carcinoma. *Histol Histopathol* 26, 71-77

21. Shaughnessy, J. (2005) Amplification and overexpression of CKS1B at chromosome band 1q21 is associated with reduced levels of p27Kip1 and an aggressive clinical course in multiple myeloma. *Hematology* 10 Suppl 1, 117-126

22. Shi, L., Wang, S., Zangari, M., Xu, H., Cao, T. M., Xu, C., Wu, Y., Xiao, F., Liu, Y., Yang, Y., Salama, M., Li, G., Tricot, G., and Zhan, F. (2010) Over-expression of CKS1B activates both MEK/ERK and JAK/STAT3 signaling pathways and promotes myeloma cell drug-resistance. *Oncotarget* 1, 22-33

23. Beroukhim, R., Getz, G., Nghiemphu, L., Barretina, J., Hsueh, T., Linhart, D., Vivanco, I., Lee, J. C., Huang, J. H., Alexander, S., Du, J., Kau, T., Thomas, R. K., Shah, K., Soto, H., Perner, S., Prensner, J., Debiasi, R. M., Demichelis, F., Hatton, C., Rubin, M. A., Garraway, L. A., Nelson, S. F., Liau, L., Mischel, P. S., Cloughesy, T. F., Meyerson, M., Golub, T. A., Lander, E. S., Mellinghoff, I. K., and Sellers, W. R. (2007) Assessing the significance of chromosomal aberrations in cancer: methodology and application to glioma. *Proc Natl Acad Sci U S A* 104, 20007-20012

24. Beroukhim, R., Mermel, C. H., Porter, D., Wei, G., Raychaudhuri, S., Donovan, J., Barretina, J., Boehm, J. S., Dobson, J., Urashima, M., Mc Henry, K. T., Pinchback, R. M., Ligon, A. H., Cho, Y. J., Haery, L., Greulich, H., Reich, M., Winckler, W., Lawrence, M. S., Weir, B. A., Tanaka, K. E., Chiang, D. Y., Bass, A. J., Loo, A., Hoffman, C., Prensner, J., Liefeld, T., Gao, Q., Yecies, D., Signoretti, S., Maher, E., Kaye, F. J., Sasaki, H., Tepper, J. E., Fletcher, J. A., Tabernero, J., Baselga, J., Tsao, M. S., Demichelis, F., Rubin, M. A., Janne, P. A., Daly, M. J., Nucera, C., Levine, R. L., Ebert, B. L., Gabriel, S., Rustgi, A. K., Antonescu, C. R., Ladanyi, M., Letai, A., Garraway, L. A., Loda, M., Beer, D. G., True, L. D., Okamoto, A., Pomeroy, S. L., Singer, S., Golub, T. R., Lander, E. S., Getz, G., Sellers, W. R., and Meyerson, M. (2010) The landscape of somatic copy-number alteration across human cancers. *Nature* 463, 899-905

25. Network, C. G. A. R. (2008) Comprehensive genomic characterization defines human glioblastoma genes and core pathways. *Nature* 455, 1061-1068

26. Garcia, D. M., Baek, D., Shin, C., Bell, G. W., Grimson, A., and Bartel, D. P. (2011) Weak seed-pairing stability and high target-site abundance decrease the proficiency of lsy-6 and other microRNAs. *Nat Struct Mol Biol* 18, 1139-1146

27. Lewis, B. P., Burge, C. B., and Bartel, D. P. (2005) Conserved seed pairing, often flanked by adenosines, indicates that thousands of human genes are microRNA targets. *Cell* 120, 15-20

28. Fujita, Y., Yagishita, S., Hagiwara, K., Yoshioka, Y., Kosaka, N., Takeshita, F., Fujiwara, T., Tsuta, K., Nokihara, H., Tamura, T., Asamura, H., Kawaishi, M., Kuwano, K., and Ochiya, T. (2015) The clinical relevance of the miR-197/CKS1B/STAT3-mediated PD-L1 network in chemoresistant non-small-cell lung cancer. *Mol Ther* 23, 717-727

29. Wang, X. C., Tian, J., Tian, L. L., Wu, H. L., Meng, A. M., Ma, T. H., Xiao, J., Xiao, X. L., and Li, C. H. (2009) Role of Cks1 amplification and overexpression in breast cancer. *Biochem Biophys Res Commun* 379, 1107-1113

30. Agarwal, V., Bell, G. W., Nam, J. W., and Bartel, D. P. (2015) Predicting effective microRNA target sites in mammalian mRNAs. *Elife* 4

31. Lembo, A., Di Cunto, F., and Provero, P. (2012) Shortening of 3'UTRs correlates with poor prognosis in breast and lung cancer. *PLoS One* 7, e31129

32. Mayr, C., and Bartel, D. P. (2009) Widespread shortening of 3'UTRs by alternative cleavage and polyadenylation activates oncogenes in cancer cells. *Cell* 138, 673-684

33. An, Y., Zhang, Z., Shang, Y., Jiang, X., Dong, J., Yu, P., Nie, Y., and Zhao, Q. (2015) miR-23b-3p regulates the chemoresistance of gastric cancer cells by targeting ATG12 and HMGB2. *Cell Death Dis* 6, e1766

34. Gao, P., Tchernyshyov, I., Chang, T. C., Lee, Y. S., Kita, K., Ochi, T., Zeller, K. I., De Marzo, A. M., Van Eyk, J. E., Mendell, J. T., and Dang, C. V. (2009) c-Myc suppression of miR-23a/b enhances mitochondrial glutaminase expression and glutamine metabolism. *Nature* 458, 762-765

35. Guo, J., Xia, B., Meng, F., and Lou, G. (2013) miR-137 suppresses cell growth in ovarian cancer by targeting AEG-1. *Biochem Biophys Res Commun* 441, 357-363

36. Li, P., Ma, L., Zhang, Y., Ji, F., and Jin, F. (2014) MicroRNA-137 down-regulates KIT and inhibits small cell lung cancer cell proliferation. *Biomed Pharmacother* 68, 7-12

37. Li, X., Liu, X., Xu, W., Zhou, P., Gao, P., Jiang, S., Lobie, P. E., and Zhu, T. (2013) c-MYC-regulated miR-23a/24-2/27a cluster promotes mammary carcinoma cell invasion and hepatic metastasis by targeting Sprouty2. *J Biol Chem* 288, 18121-18133

38. Smith, A. R., Marquez, R. T., Tsao, W. C., Pathak, S., Roy, A., Ping, J., Wilkerson, B., Lan, L., Meng, W., Neufeld, K. L., Sun, X. F., and Xu, L. (2015) Tumor suppressive microRNA-137 negatively regulates Musashi-1 and colorectal cancer progression. *Oncotarget* 6, 12558-12573

39.   Zaman, M. S., Thamminana, S., Shahryari, V., Chiyomaru, T., Deng, G., Saini, S., Majid, S., Fukuhara, S., Chang, I., Arora, S., Hirata, H., Ueno, K., Singh, K., Tanaka, Y., and Dahiya, R. (2012) Inhibition of PTEN gene expression by oncogenic miR-23b-3p in renal cancer. *PLoS One* 7, e50203

40.   Zhu, X., Li, Y., Shen, H., Li, H., Long, L., Hui, L., and Xu, W. (2013) miR-137 inhibits the proliferation of lung cancer cells by targeting Cdc42 and Cdk6. *FEBS Lett* 587, 73-81

41.   Di Leva, G., Garofalo, M., and Croce, C. M. (2014) MicroRNAs in cancer. *Annu Rev Pathol* 9, 287-314

42.   Kasinski, A. L., and Slack, F. J. (2011) Epigenetics and genetics. MicroRNAs en route to the clinic: progress in validating and targeting microRNAs for cancer therapy. *Nat Rev Cancer* 11, 849-864

Figure Legends
FIGURE 1. Regulation of KDM4A by miRNA. *A*, Schematic of KDM4A 3'UTR. The length in base pairs and the positions of TARGETSCAN 6.2 predicted seed sequences are indicated. The seed sequences are indicated as are the mutations performed to generate the mutant 3'-UTR (MT) in the schematic. *B*, Western blot analysis of KDM4A protein levels following treatment with the indicated miRNA mimics. Representative western from one of two biological replicates. *C*, Western blot analysis of KDM4A protein levels following treatment with the indicated miRNA inhibitors (anti-miRs). Representative western from one of two biological replicates. *D*, Luciferase analysis of KDM4A WT and KDM4A MT 3'-UTR response to miRNA mimics. Data were normalized to the co-transfected β-galactosidase levels for relative light units. Data represent average of two biological replicates assayed in technical triplicates. Error bars represent the S.E.M. * indicates significant difference from CTRL by two-tailed Student's *t-test* (p<0.05).

FIGURE 2. Regulation of KDM4A by miRNAs promotes copy gain. *A*, Western blot analysis of KDM4A levels in response to miRNA inhibitors in RPE cells. Representative western from one of two biological replicates. *B*, Treatment of RPE cells with the indicated anti-miRs does not affect cell cycle distribution. Representative cell cycle distribution from one of two biological replicates. *C*, Representative images of FISH for 1q12h and 8c in anti-miR treated RPE cells. Note the increased number of 1q12h foci (indicated by green chevrons), but not chromosome 8c foci (indicated by red chevrons) in the anti-miR treated cells. Scale bars represent 5µm. *D*, Treatment of RPE cells with anti-miRs induces copy gain of 1q12-21. Quantification of FISH analysis. Data represent the average of two biological replicates. Error bars represent the S.E.M. * indicates significant difference from CTRL by two-tailed Student's *t-test* (p<0.05). *E*, Western blot analysis of KDM4A levels in response to miRNA inhibitors in MDA-MB-231 cells. Representative western from one of two biological replicates. *F*, Steady state *KDM4A* transcript levels do not change in response to miRNA inhibitors in MDA-MB-231 cells. Data represent the average of two biological replicates. Error bars represent the S.E.M. * indicates significant difference from CTRL by two-tailed Student's *t-test* (p<0.05). *G*, Cell cycle distribution of MDA-MB-231 cells treated with anti-mirs. Representative distribution from one of two biological replicates. *H*, Treatment of MDA-MB-231 cells with anti-miRs induces copy gain of 1q12h. Quantification of FISH analysis. Data represent the average of two biological replicates. Error bars represent the S.E.M. * indicates significant difference from CTRL by two-tailed Student's *t-test* (p<0.05). *I*, Western blot analysis of KDM4A levels in response to miRNA inhibitors in SK-N-AS neuroblastoma cells. Representative western from one of two biological replicates. *J*, Treatment of SK-N-AS cells with anti-miRs induces copy gain of 1q12h. Quantification of FISH analysis. Data represent the average of two biological replicates. Error bars represent the S.E.M. * indicates significant difference from CTRL by two-tailed Student's *t-test* (p<0.05). *K*, Western blot analysis of KDM4A levels in response to miRNA inhibitors in H2591 lung cancer cells. Representative western from one of two biological replicates. *L*, Treatment of H2591 cells with anti-miRs induces copy gain of 1q12h. Quantification of FISH analysis. Data represent the average of two biological replicates. Error bars represent the S.E.M. * indicates significant difference from CTRL by two-tailed Student's *t-test* (p<0.05).

FIGURE 3. MicroRNA-dependent regulation of KDM4A promotes TSSG. *A*, Western blot depicting KDM4A levels in asynchronous or hydroxyurea (HU) arrested and released cells treated with miRNA inhibitors. Representative western from one of two biological replicates. *B*, Copy gain induced by miRNA inhibitors is transient. Quantification of FISH analysis from of asynchronous RPE cells (Asyn), or HU arrested (HU 0) or HU released for four hours (HU 4). Data represent the average of two biological replicates. Error bars represent the S.E.M. * indicates significant difference from untreated CTRL by two-tailed Student's *t-test* (p<0.05). *C-E*, Treatment of RPE cells with the indicated anti-miRs does not affect cell cycle distribution (*C*) or
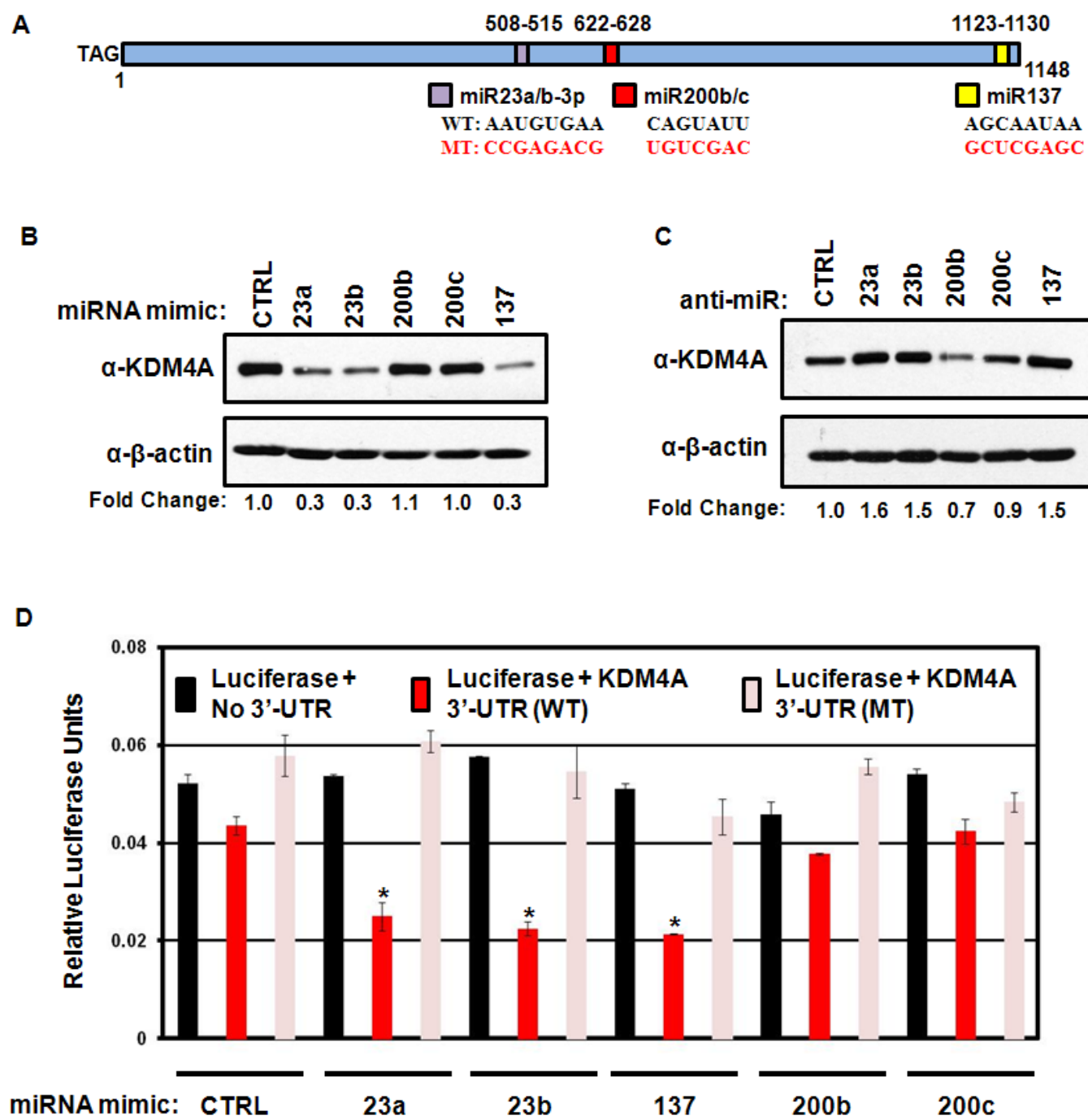
HU arrest (*D*) or HU release (*E*). Representative cell cycle profiles from one of two biological replicates.
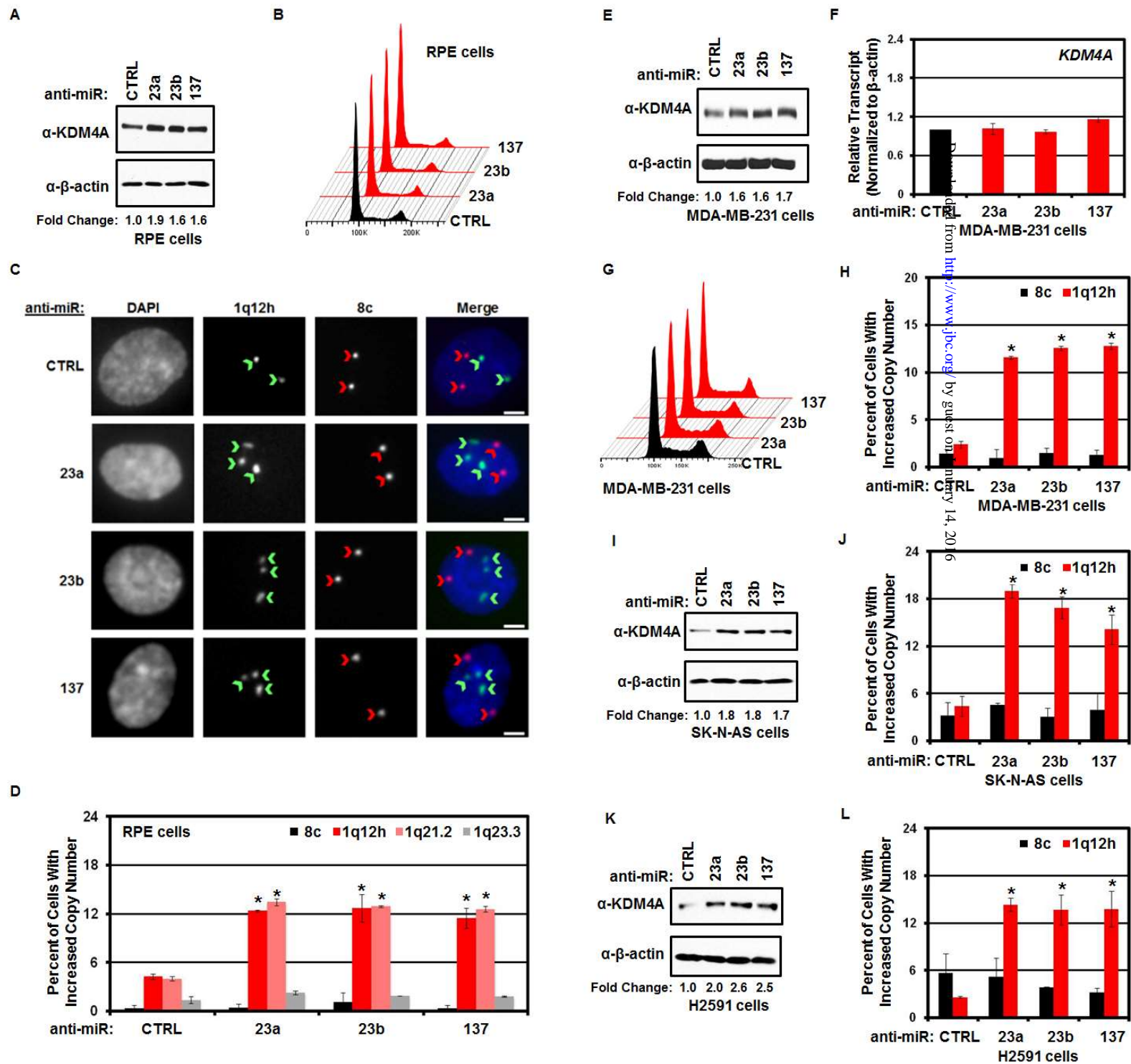
FIGURE 4. Regulation of TSSG by miRNA is KDM4A-dependent. *A*, Western blot depicting KDM4A levels from combined anti-miR and KDM4A depletion. Representative western from one of two biological replicates. *B*, Treatment of RPE cells with the indicated anti-miRs and siRNAs does not affect cell cycle distribution. Representative cell cycle distribution from one of two biological replicates. *C*, TSSG induced by miRNA inhibitor treatment is KDM4A-dependent. Quantification of FISH analysis. Data represent the average of two biological replicates. Error bars represent the S.E.M. * indicates significant difference from CTRL by two-tailed Student's *t-test* (p<0.05). † indicates significant difference from corresponding anti-miR treated with siCTRL by two-tailed Student's *t-test* (p<0.05) but not significantly different from anti-miR CTRL/siCTRL.

FIGURE 5. Increased MicroRNA expression can ablate hypoxia-dependent TSSG.
A, Western blot depicting inhibition of hypoxia-dependent KDM4A induction using miRNA mimics. Representative western from one of two biological replicates. *B*, Cell cycle distribution of RPE cells treated with anti-mirs. Representative cell cycle distribution from one of two biological replicates. *C*, Quantification of FISH analysis of TSSG in hypoxia-treated cells following miRNA mimic treatment. Data represent the average of two biological replicates. Error bars represent the S.E.M. * indicates significant difference from Normoxia CTRL by two-tailed Student's *t-test* (p<0.05). † indicates significant difference from Hypoxia CTRL by two-tailed Student's *t-test* (p<0.05) but not significantly different from the Normoxia CTRL.
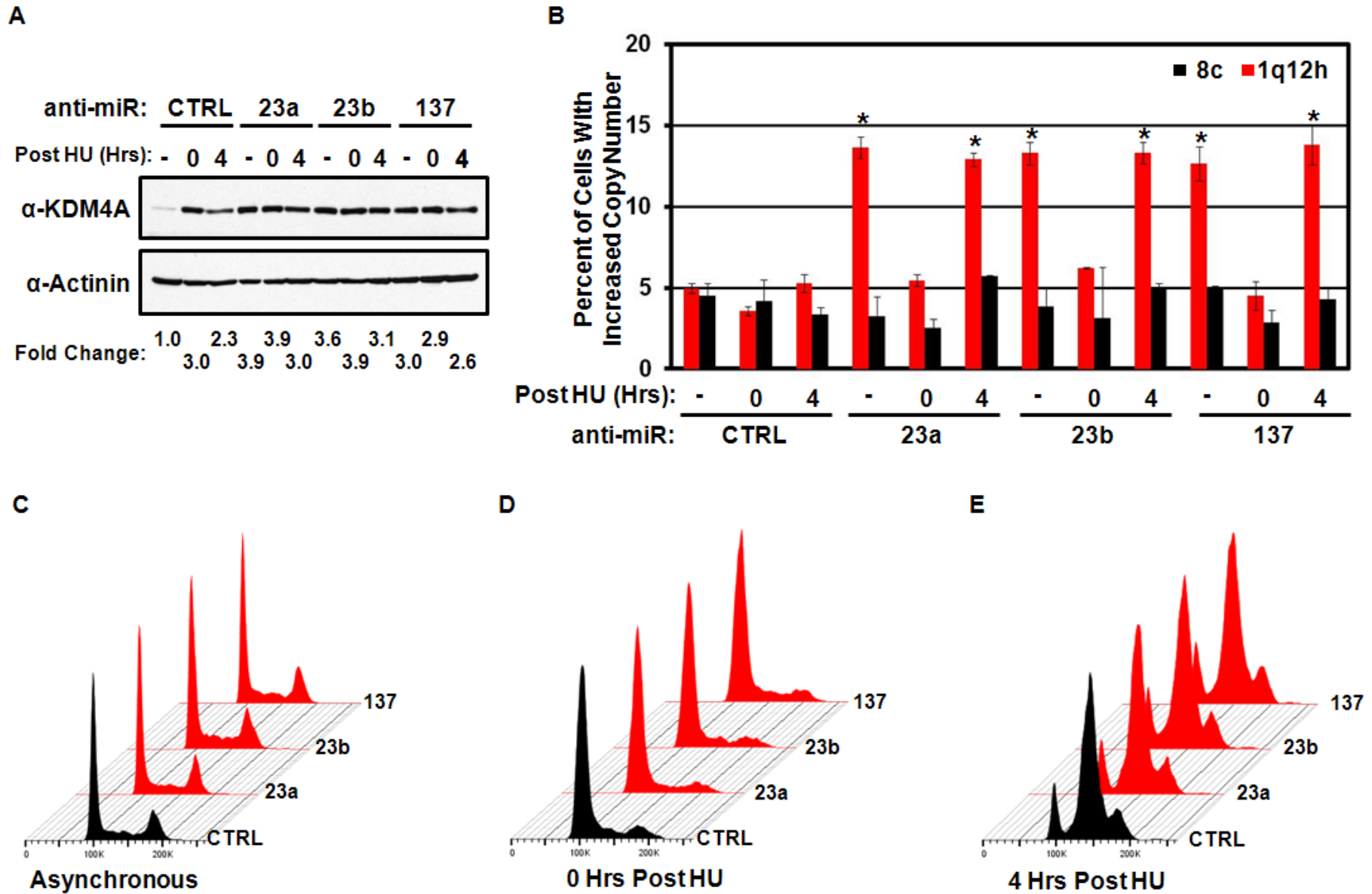
FIGURE 6. Hsa-mir-23a loss in breast cancer correlates with 1q12-21 copy gain and *CKS1B* expression. *A*, TCGA primary breast tumor samples with loss of hsa-mir-23a have an enrichment for copy gain of 1p11.2 through 1q23.3 (blue shaded region). Dashed blue line indicates genomic location of the indicated miRNA. *B,* TCGA primary breast tumor samples with loss of hsa-mir-137 have enrichment for copy gain of 1p11.2 through 1q23.3 (blue shaded region). Dashed blue line indicates genomic location of the indicated miRNA. *C,D*, Expression of the drug resistance oncogene *CKS1B* is increased in tumors with loss of hsa-mir-23a (*C*) or gain of KDM4A (*D*). The wilcoxon p-value is indicated in each box-plot.

FIGURE 7. Regulation of *CKS1B* copy number and expression by miRNAs correlates with a reduced response to cisplatin. (*A*) Treatment of MDA-MB-231 cells with anti-miRs induces copy gain of *CKS1B*, but not the control region *CDKN2C*. Quantification of FISH analysis. Data represent the average of two biological replicates. Error bars represent the S.E.M. * indicates significant difference from CTRL by two-tailed Student's *t-test* (p<0.05). *B*, Treatment of MDA-MB-231 cells with anti-miRs induces expression of *CKS1B*. Data represent the average of two biological replicates. Error bars represent the S.E.M. * indicates significant difference from CTRL by two-tailed Student's *t-test* (p<0.05). *C*, Treatment of MDA-MB-231 cells with anti-miRs reduced the response to 300 µM cisplatin. Cells were plated and transfected with the indicated anti-miRs. 24 hours later vehicle (0.9% NaCl) or 300 µM cisplatin was added. Cell survival was measured 48 hours later by MTT assay. Data represent the average of eight biological replicates measured in technical quadruplicate. Error bars represent the S.E.M. * indicates significant difference from CTRL by two-tailed Student's *t-test* (p<0.05). *D,* Targetscan 7.0 UTR schematic depicting reduced read count at KDM4A 3'-UTR, which would remove hsa-mir-137 seed sequence in some transcripts. Adapted from TARGETSCAN 7.0.

A

508-515 622-628   1123-1130

TAG [   ] 1148
1

■ miR23a/b-3p   ■ miR200b/c   ■ miR137

WT: AAUGUGAA   CAGUAUU   AGCAAUAA
MT: CCGAGACG   UGUCGAC   GCUCGAGC

B

miRNA mimic: CTRL 23a 23b 200b 200c 137

α-KDM4A

α-β-actin

Fold Change: 1.0 0.3 0.3 1.1 1.0 0.3

C

anti-miR: CTRL 23a 23b 200b 200c 137

α-KDM4A

α-β-actin

Fold Change: 1.0 1.6 1.5 0.7 0.9 1.5

D

■ Luciferase +   ■ Luciferase + KDM4A   ■ Luciferase + KDM4A
  No 3'-UTR   3'-UTR (WT)   3'-UTR (MT)

miRNA mimic: CTRL   23a   23b   137   200b   200c

A

anti-miR: CTRL 23a 23b 137

α-KDM4A

α-β-actin

Fold Change: 1.0 1.9 1.6 1.6
RPE cells

B

RPE cells

137
23b
23a
CTRL

0   100K   200K

C

anti-miR: DAPI   1q12h   8c   Merge

CTRL

23a

23b

137

D

RPE cells   ■ 8c ■ 1q12h ■ 1q21.2 ■ 1q23.3

anti-miR: CTRL   23a   23b   137

Percent of Cells With Increased Copy Number

E

anti-miR: CTRL 23a 23b 137

α-KDM4A

α-β-actin

Fold Change: 1.0 1.6 1.6 1.7
MDA-MB-231 cells

F

KDM4A

Relative Transcript (Normalized to β-actin)

anti-miR: CTRL   23a   23b   137
MDA-MB-231 cells

G

137
23b
23a
CTRL

0   100K   150K   250K

MDA-MB-231 cells

H

■ 8c ■ 1q12h

anti-miR: CTRL   23a   23b   137
MDA-MB-231 cells

Percent of Cells With Increased Copy Number

I

anti-miR: CTRL 23a 23b 137

α-KDM4A

α-β-actin

Fold Change: 1.0 1.8 1.8 1.7
SK-N-AS cells

J

■ 8c ■ 1q12h

anti-miR: CTRL   23a   23b   137
SK-N-AS cells

Percent of Cells With Increased Copy Number

K

anti-miR: CTRL 23a 23b 137

α-KDM4A

α-β-actin

Fold Change: 1.0 2.0 2.6 2.5
H2591 cells

L

■ 8c ■ 1q12h

anti-miR: CTRL   23a   23b   137
H2591 cells

Percent of Cells With Increased Copy Number

Black Figure 3

A

anti-miR: CTRL 23a 23b 137

Post HU (Hrs): - 0 4 - 0 4 - 0 4 - 0 4

α-KDM4A

α-Actinin

Fold Change: 1.0 2.3 3.9 3.6 3.1 2.9
3.0 3.9 3.0 3.9 3.0 2.6

B

C

Asynchronous

D

0 Hrs Post HU

E

4 Hrs Post HU

A

siCTRL   siKDM4A

anti-miR: CTRL   23a   23b   137   CTRL   23a   23b   137

α-KDM4A

α-β-actin

Fold Change: 1.0   2.3   2.5   2.4   0.3   1.1   1.1   1.1

B

137
23b
23a
CTRL   siKDM4A
137
23b
23a
CTRL   siCTRL

0   100K   200K

C

■ 8c   ■ 1q12h

Percent of Cells With Increased Copy Number

anti-miR: CTRL   23a   23b   137   CTRL   23a   23b   137

siCTRL   siKDM4A

A

Hypoxia

miRNA mimic: CTRL | CTRL | 23a | 23b | 137

α-KDM4A

α-β-actin

Fold Change: 1.0 3.7 1.2 1.1 0.8

α-CAIX

α-Actinin

B

137 1% O_2

23b 1% O_2

23a 1% O_2

CTRL 1% O_2

CTRL Normoxia

0   100K   200K

C

■ 8c ■ 1q12h

Percent of Cells With Increased Copy Number

Pre-miR: CTRL | CTRL | 23a | 23b | 137

Hypoxia

A

hsa-mir-23a , p.gaussian ; Cytoband Copy in hsa-mir-23a Loss Compared to hsa-mir-23a Wild samples

BRCA Cancer
hsa-mir-23a-Loss: 33
hsa-mir-23a-WT: 304

B

hsa-mir-137 , p.gaussian ; Cytoband Copy in hsa-mir-137 Loss Compared to hsa-mir-137 Wild samples

BRCA Cancer
hsa-mir-137-Loss: 25
hsa-mir-137-WT: 304

C

BRCA

p=8.98e^{-05}

Loss
(N= 33)

No Change
(N= 304)

Hsa-mir-23a Copy Number

D

BRCA

p=0.00014

Gain
(N= 11)

No Change
(N= 304)

KDM4A Copy Number

Black Figure 7

A — Percent of Cells With Increased Copy Number; legend: ■ *CDKN2C* ■ *CKS1B*; x-axis anti-miR: CTRL, 23a, 23b, 137

B — Relative Transcript (Normalized to β-actin); *CKS1B*; x-axis anti-miR: CTRL, 23a, 23b, 137

C — Relative Cell Viability (to 0 µM Cisplatin); legend: ■ 0 µM ■ 300 µM; x-axis anti-miR: CTRL, 23a, 23b, 137

D — Human KDM4A ENST00000372396.3 3' UTR length: 1148 — ENST00000372396.3

■ hsa-mir-23-3p   ■ hsa-mir-137

Access the most updated version of this article at doi: 10.1074/jbc.M115.711648

Find articles, minireviews, Reflections and Classics on similar topics on the JBC Affinity Sites.

Alerts:

- When this article is cited
- When a correction for this article is posted

Click here to choose from all of JBC's e-mail alerts

This article cites 0 references, 0 of which can be accessed free at
http://www.jbc.org/content/early/2016/01/11/jbc.M115.711648.full.html#ref-list-1